Supplementary Information

Microphase-optimized sulfonated poly(biphenyl-piperidine-alkylene)-co-poly(biphenyl-trifluoroacetophenylene) proton exchange membranes with enhanced proton conductivity and oxidative stability for water electrolysis

*Thi Cam Thach To, Anh Le Mong and Dukjoon Kim**

T.C.T. To, A.L. Mong, Prof. D. Kim

School of Chemical Engineering, Sungkyunkwan University, Suwon, Gyeonggi-do, 16419, Republic of Korea

E-mail: djkim@skku.edu

Number of figures: 7

Number of pages: 16

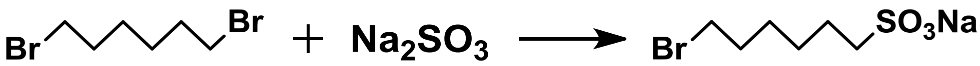

Figure S1. Synthetic pathway of sodium 6-bromohexanesulfonate (Br-6-SO_3Na).

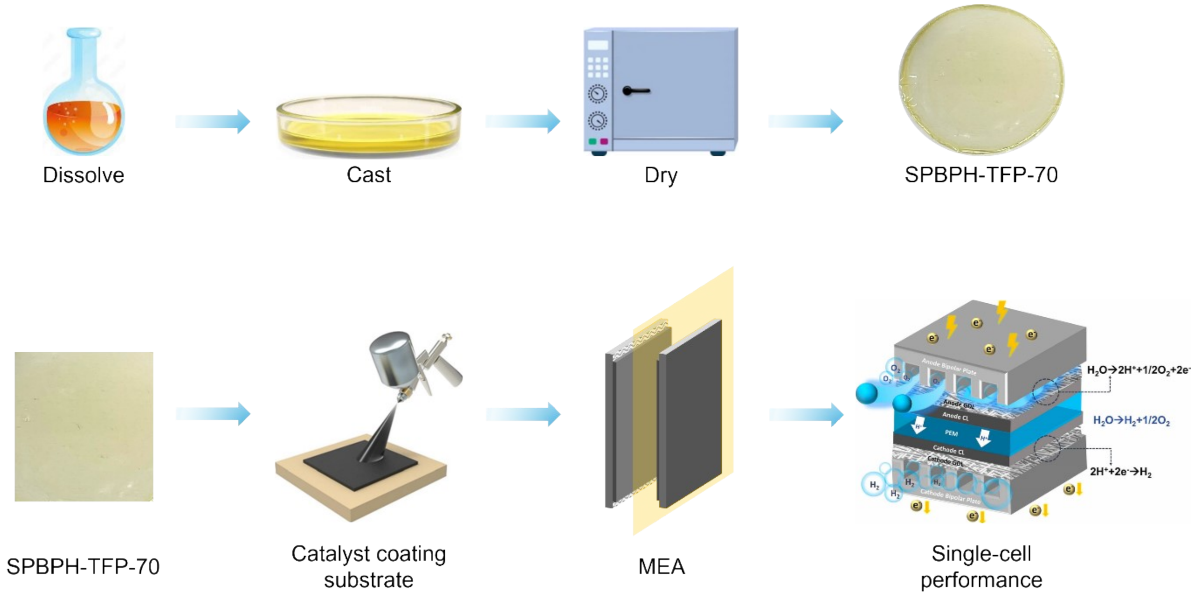

Figure S2. Membrane electrode assembly (MEA) preparation for single-cell performance.

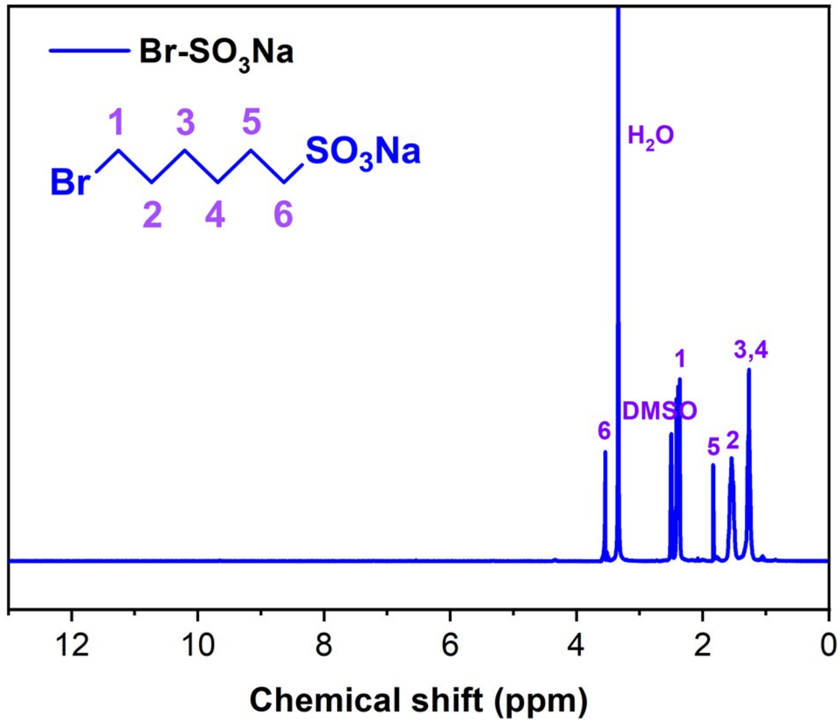

Figure S3. [1]H-NMR spectra of sodium 6-bromohexanesulfonate (Br-6-SO_3Na).

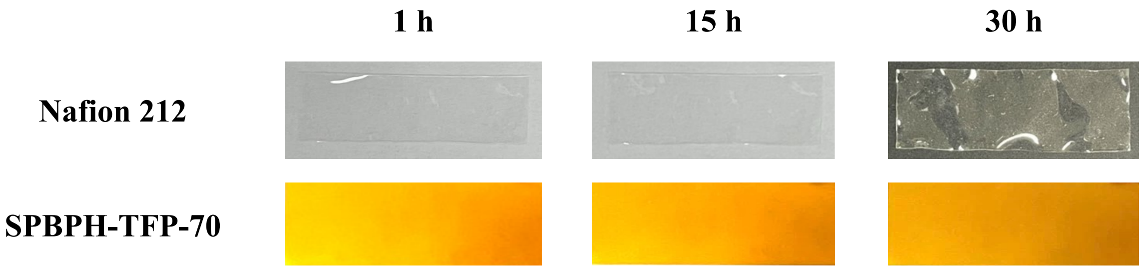

Figure S4. Visual appearance of Nafion 212 and SPBPH-TFP-70 membranes after 1 h, 15 h, and 30 h exposure to Fenton's reagent (3 wt.% H_2O_2, 4 ppm Fe^{2+}) at 80 ^{o}C.

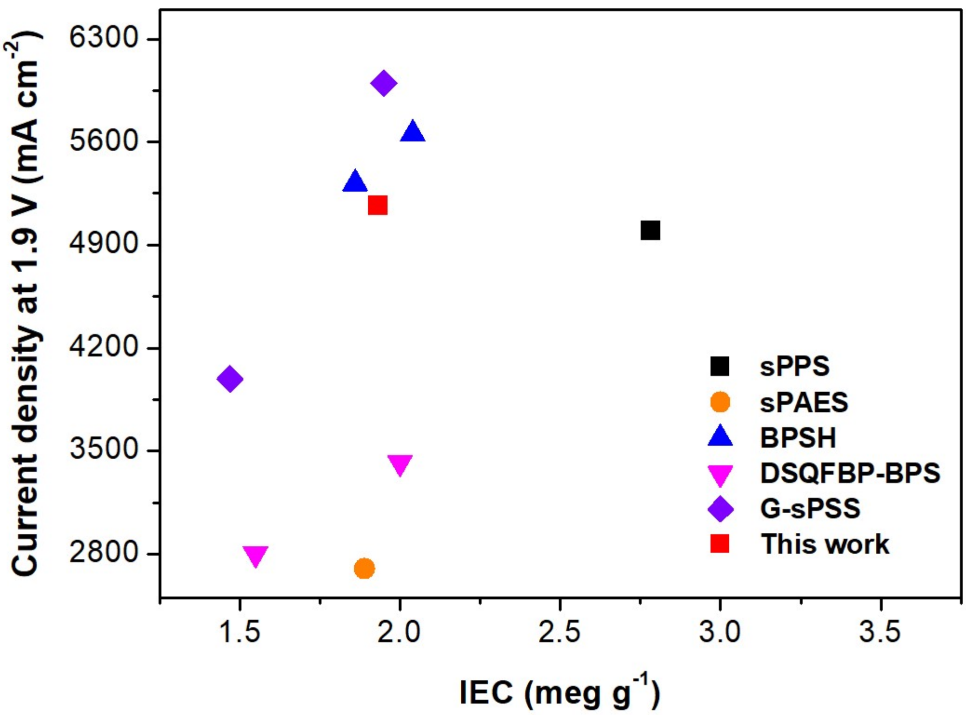

Figure S5. Comparison of proton exchange membrane water electrolysis (PEMWE) current densities at 1.9 V versus ion exchange capacity (IEC), with reported recent studies.

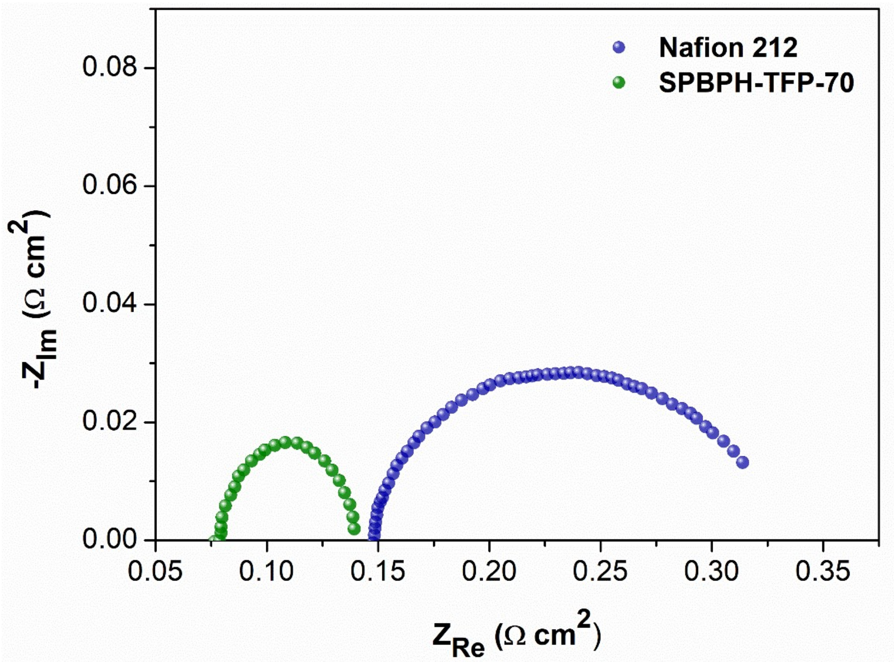

Figure S6. Nyquist plot of PEMWE cells using SPBPH-TFP-70 and Nafion 212 membranes under 1 A cm^{-2} at 30 ^{o}C.

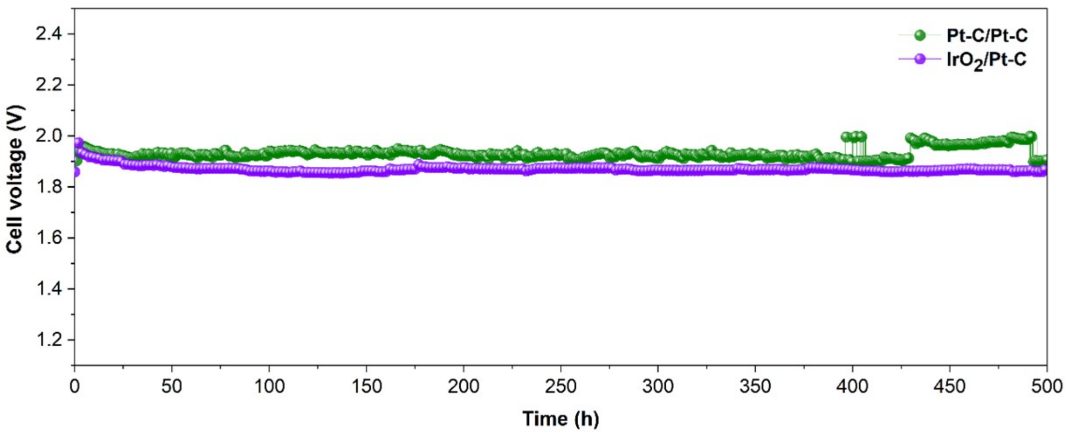

Figure S7. Long-term stability test of the SPBPH-TFP-70 cells using Pt-C/Pt-C and IrO_2/Pt-C as the anode/cathode catalyst materials, respectively, under 1 A cm^{-2} at 60 ^{o}C for 500 h of proton exchange membrane water electrolysis (PEMWE) operation.

Table S1. Root-mean-square (RMS) surface roughness of SPBPH-TFP-x (x = 60, 70, 80, 90).

PEM	Mean height (nm)	RMS roughness (R_q, nm)	Average roughness (R_a, nm)
SPBPH-TFP-60	8.13	7.32	5.12
SPBPH-TFP-70	7.68	5.47	4.25
SPBPH-TFP-80	7.12	4.89	3.78
SPBPH-TFP-90	6.75	4.15	3.21

Table S2. IEC, WU, and λ of the SPBPH-TFP-x (x = 60, 70, 80, 90) PEMs.

PEM	IEC (meg g^{-1})	WU (%)	λ
SPBPH-TFP-60	1.57	20.63	7.30
SPBPH-TFP-70	1.75	25.36	8.05
SPBPH-TFP-80	1.96	30.71	8.71
SPBPH-TFP-90	2.17	37.19	9.53

The hydration number (λ) was calculated from the following formula:

$$\lambda = \frac{WU\ (\%) \times 10}{IEC \times 18} \tag{S-1}$$

Table S3. Mechanical properties of the SPBPH-TFP-x (x = 60, 70, 80, 90) at the dry state.

PEM	Tensile strength (MPa)	Elongation at break (%)	Young's modulus (GPa)
SPBPH-TFP-60	87.6 ± 1.0	10.5 ± 0.3	2.0 ± 0.0045
SPBPH-TFP-70	83.5 ± 0.2	13.5 ± 0.4	1.3 ± 0.0033
SPBPH-TFP-80	75.1 ± 0.6	16.5 ± 0.7	1.0 ± 0.0025
SPBPH-TFP-90	65.0 ± 0.3	21.0 ± 0.5	0.7 ± 0.0021

Table S4. Mechanical properties of the SPBPH-TFP-x (x = 60, 70, 80, 90) at the wet state.

PEM	Tensile strength (MPa)	Elongation at break (%)	Young's modulus (GPa)
SPBPH-TFP-60	34.6 ± 0.1	21.7 ± 0.1	1.5 ± 0.0096
SPBPH-TFP-70	26.2 ± 0.1	27.1 ± 0.2	1.1 ± 0.0012
SPBPH-TFP-80	26.3 ± 0.2	30.8 ± 0.3	0.8 ± 0.0011
SPBPH-TFP-90	22.5 ± 0.1	41.9 ± 0.2	0.5 ± 0.0015

Table S5. Comparison of PEMWE performance with reported values.

PEM	IEC (meg g^{-1})	Anode/ cathode catalyst	Catalyst loading (mg cm^{-2})	Temperature (^oC)	Current density (mA cm^{-2})			Ref.
					1.6 V	1.8 V	1.9 V	
SPBPH-TFP-70	***1.93***	***Pt-C/Pt-C***	***1.0/0.4***	***90***	***1750***	***3920***	***5170***	***This work***
SPAES	1.89	IrO_2/Pt-C	2.0/0.4	90	1070	2210	2700	[1]
BPSH50	1.86	IrO_2/Pt-C	2.0/0.4	80	1410	3890	5320	[2]
BPSH60	2.04	IrO_2/Pt-C	2.0/0.4	80	1460	4210	5656	[2]
Nafion 212	0.91	IrO_2/Pt-C	2.0/0.4	90	540	1660	2840	[3]
DSQFBP-BPS 10k-5k	2.00	IrO_2/Pt-C	1.0/0.4	90	750	2320	3420	[3]
DSQFBP-BPS 10k-10k	1.55	IrO_2/Pt-C	1.0/0.4	90	680	1950	2800	[3]
G-sPSS-1.47	1.47	IrO_2/Pt-C	2.0/0.4	90	1140	3050	3990	[4]
G-sPSS-1.95	1.95	IrO_2/Pt-C	2.0/0.4	90	2480	5060	6000	[4]
sPPS	2.78	IrO_2/Pt-C	1.5/0.5	80	890	3480	5000	[5]
Nafion 115	-	IrO_2/Pt-C	1.5/0.5	80	0.5	1.5	2.0	[5]
Nafion-CNT@SiO_2	1.01	IrO_2/Pt-C	1.0/0.4	80	1	2560	3.188	[6]
Reinforced R98-05S	-	$IrRuO_x$/Pt-C	0.37/0.1	90	2.0	5000	6.6	[7]
Nafion 117	0.93	IrO_2/Pt-C	2.0/0.4	80	0.53	1.167	3.20	[8]
Nafion 115	-	Ir/Pt-C	0.14/0.4	80	0.875	2.0	2.2	[9]
Nafion 117	-	Ir black/Pt-C	2.0/2.0	75	0.5	1.083	1.375	[10]
Nafion 212	-	Ir/Pt	2.0/1.0	80	0.875	2.75	3.813	[11]
Aquivion	-	IrO_2/Pt-C	2.0/0.3	90	1.1	3.2	3.6	[12]
Aquivion E87-12S	-	IrO_2/Pt	2.0/2.0	60	0.688	2.375	3.375	[13]
PFSA/ssPS	1.05	IrO_{x-}ATO/Pt-carbon nanofiber	1.0/0.4	80	0.25	1.125	1.625	[14]

References

[1] Park, J. E.; Kim, J.; Han, J.; Kim, K.; Park, S.; Kim, S.; Park, H. S.; Cho, Y.-H.; Lee, J. C.; Sung, Y.-E. High-performance proton-exchange membrane water electrolysis using a sulfonated poly(arylene ether sulfone) membrane and ionomer. Journal of Membrane Science 2021, 620, 118871. DOI: https://doi.org/10.1016/j.memsci.2020.118871.

[2] Han, S.-Y.; Yu, D. M.; Mo, Y.-H.; Ahn, S. M.; Lee, J. Y.; Kim, T.-H.; Yoon, S. J.; Hong, S.; Hong, Y. T.; So, S. Ion exchange capacity controlled biphenol-based sulfonated poly(arylene ether sulfone) for polymer electrolyte membrane water electrolyzers: Comparison of random and multi-block copolymers. Journal of Membrane Science 2021, 634, 119370. DOI: https://doi.org/10.1016/j.memsci.2021.119370.

[3] Chae, J. E.; Lee, S. Y.; Baek, S. Y.; Song, K. H.; Park, C. H.; Kim, H.-J.; Lee, K.-S. High-performance multiblock PEMs containing a highly acidic fluorinated-hydrophilic domain for water electrolysis. Journal of Membrane Science 2021, 638, 119694. DOI: https://doi.org/10.1016/j.memsci.2021.119694.

[4] Ahn, S. M.; Park, J. E.; Jang, G. Y.; Jeong, H. Y.; Yu, D. M.; Jang, J. K.; Lee, J.-C.; Cho, Y.-H.; Kim, T.-H. Highly Sulfonated Aromatic Graft Polymer with Very High Proton Conductivity and Low Hydrogen Permeability for Water Electrolysis. Journal of ACS Energy Letters 2022, 7, 4427−4435. DOI: https://doi.org/10.1021/acsenergylett.2c02143.

[5] Klose, C.; Saatkamp, T.; Münchinger, A.; Bohn, L.; Titvinidze, G.; Breitwieser, M.; Kreuer, K.-D.; Vierrath, S. All-Hydrocarbon MEA for PEM Water Electrolysis Combining Low Hydrogen Crossover and High Efficiency. Advanced Energy Materials 2020, 10 (14), 1903995, DOI: https://doi.org/10.1002/aenm.201903995.

[6] Huang, M.; Li, Y.; Lu, H.; Gao, S.; Kwofie, F.; Guo, X.; Meyer, Q.; Wang, Y.; Zhao, C.; Li, N.; Cheng, Y. Construction of efficient proton channels with silica-encapsulated carbon nanotubes for proton exchange membrane water electrolysers. Chemical Engineering Journal 2025, 522, 167557. DOI: https://doi.org/10.1016/j.cej.2025.167557.

[7] Siracusano, S.; Panto, F.; Tonella, S.; Oldani, C.; Arico, A. S. Reinforced short-side-chain Aquivion® membrane for proton exchange membrane water electrolysis. International Journal

of Hydrogen Energy 2022, 47, 15557−15570. DOI: https://doi.org/10.1016/j.ijhydene.2022.03.061.

[8] Lee, C. J.; Song, J.-H.; Yoon, K. S.; Rho, Y.-C.; Yu, D. M.; Oh, K.-H.; Lee, J. Y.; Kim, T.-H.; Hong, Y. T.; Kim, H.-J.; Yoon, S. J.; So, S.-Y. Controlling hydrophilic channel alignment of perfluorinated sulfonic acid membranes via biaxial drawing for high performance and durable polymer electrolyte membrane water electrolysis. Journal of Power Sources 2022, 518, 230772. DOI: https://doi.org/10.1016/j.jpowsour.2021.230772.

[9] Jiang, G.; Yu, H.; Li, Y.; Yao, D.; Chi, J.; Sun, S.; Shao, Z. Low-Loading and Highly Stable Membrane Electrode Based on an Ir@WOxNR Ordered Array for PEM Water Electrolysis. ACS Applied Materials & Interfaces 2021, 13, 15073−15082. DOI: https://doi.org/10.1021/acsami.0c20791.

[10] Kim, T.; Sihn, Y.; Yoon, I.-H.; Yoon, S. J.; Lee, K.; Yang, J. H.; So, S.; Park, C. W. Monolayer Hexagonal Boron Nitride Nanosheets as Proton Conductive Gas Barriers for Polymer Electrolyte Membrane Water Electrolysis. ACS Applied Nano Materials 2021, 4, 9104−9112. DOI: https://doi.org/10.1021/acsanm.1c01691.

[11] Marocco, P.; Sundseth, K.; Aarhaug, T.; Lanzini, A.; Santarelli, M.; Oyarce Barnett, A.; Thomassen, M. Online measurements of fluoride ions in proton exchange membrane water electrolysis through ion chromatography. Journal of Power Sources 2021, 483, 229179. DOI: https://doi.org/10.1016/j.jpowsour.2020.229179.

[12] Siracusano, S.; Baglio, V.; Stassi, A.; Merlo, L.; Moukheiber, E.; Arico, A.S. Performance analysis of short-side-chain Aquivions perfluorosulfonic acid polymer for proton exchange membrane water electrolysis. Journal of Membrane Science 2014, 466, 1–7. DOI: https://doi.org/10.1016/j.memsci.2014.04.030.

[13] Siracusano, S.; Oldani, C.; Navarra, M. A.; Tonella, S.; Mazzapioda, L.; Briguglio, N.; Aricò, A. S. Chemically stabilised extruded and recast short side chain Aquivion® proton exchange membranes for high current density operation in water electrolysis. Journal of Membrane Science 2019, 578, 136–148. DOI: https://doi.org/10.1016/j.memsci.2019.02.021.

[14] Cieluch, M.; Du¨erkop, D.; Kazamer, N.; Wirkert, F.; Podleschny, P.; Rost, U.; Schmiemann, A.; Brodmann, M. Manufacturing and investigation of MEAs for PEMWE based on glass fibre reinforced PFSA/ssPS composite membranes and catalyst-coated substrates prepared via catalyst electrodeposition. International Journal of Hydrogen Energy 2024, 52, 521−533. DOI: https://doi.org/10.1016/j.ijhydene.2023.07.310.